YALE
PEABODY
MUSEUM

Journal of Marine Research

The *Journal of Marine Research,* one of the oldest journals in American marine science, published important peer-reviewed original research on a broad array of topics in physical, biological, and chemical oceanography vital to the academic oceanographic community in the long and rich tradition of the Sears Foundation for Marine Research at Yale University.

An archive of all issues from 1937 to 2021 (Volume 1–79) are available through EliScholar, a digital platform for scholarly publishing provided by Yale University Library at https://elischolar.library.yale.edu/.

Requests for permission to clear rights for use of this content should be directed to the authors, their estates, or other representatives. The *Journal of Marine Research* has no contact information beyond the affiliations listed in the published articles. We ask that you provide attribution to the *Journal of Marine Research.*

Yale University provides access to these materials for educational and research purposes only. Copyright or other proprietary rights to content contained in this document may be held by individuals or entities other than, or in addition to, Yale University. You are solely responsible for determining the ownership of the copyright, and for obtaining permission for your intended use. Yale University makes no warranty that your distribution, reproduction, or other use of these materials will not infringe the rights of third parties.

Optics of heterotrophic nanoflagellates and ciliates: A tentative assessment of their scattering role in oceanic waters compared to those of bacterial and algal cells

by André Morel[1] and Yu-Hwan Ahn[1]

ABSTRACT

Heterotrophic nanoflagellates and naked ciliates have been isolated from open sea waters and separately grown by using free living marine bacteria as food. The modal diameters of purified (by differential screening) populations are about 3 and 12.5 µm, respectively. The spectral determination of their absorption and scattering properties have been carried out. By combining these values with the cell number density and size distribution function, simultaneously measured, the efficiency factors for absorption and scattering at the level of individual cells can be derived. From these factors and by using the anomalous diffraction theory, the relative index of refraction can be derived (at least for flagellates); it agrees with the predictions made from the intracellular carbon concentrations (mean value 129 kgC m^{-3}). In addition, backscattering efficiency (not determined) is computed through Mie theory. Like bacteria, these larger protists exhibit the typical absorption maximum of cytochrome (at about 410–415 nm). The impact of these organisms upon the properties of oceanic waters is compared to that of the bacterial compartment, in terms of scattering and backscattering coefficients. For that, the bacterial number-to-chlorophyll concentration relationship, as proposed by Cole *et al.* (1988), is adopted and reasonable assumptions resting on field data are made concerning the respective biomasses of bacterioplankton and heterotrophic nanoplankton. An assessment of the comparative role of the phototrophic and heterotrophic communities is also attempted. Algal cells in open ocean, and to a lesser extent small heterotrophs, dominate the scattering coefficients; the sum of their contributions is close to the coefficient measured in various (from oligotrophic to eutrophic) waters. On the contrary, these organisms are definitely insignificant contributors to the backscattering coefficient. In the backscattering process, heterotrophic bacteria are the more efficient agents; they, however, account only for a small part of the coefficient as actually derived from measurements at sea. The main contributors would presumably be the abundant population of very tiny, poorly known particles with size similar to, or below that of commonly identified bacteria. This partly speculative conclusion, based on theoretical considerations, is supported by recent studies demonstrating the importance of submicrometer detrital particles.

1. Laboratoire de Physique & Chimie Marines, Université Pierre et Marie Curie (CNRS: UA353), B.P. 8, F 06230 Villefranche sur Mer, France.

1. Introduction

The optical properties of free-living marine bacteria and the possible impact of this trophic compartment upon the optical properties of oceanic waters have been previously examined (Morel and Ahn, 1990). Other ubiquitous heterotrophic protists, involved in the so called bacterial loop, grazing on bacteria and also on small algae, are now identified as forming an important assemblage within the nanoplanktonic community (see e.g. Azam *et al.,* 1983; Andersen and Fenchel, 1985; Rassoulzadegan and Sheldon, 1986). Less studied than their autotrophic cousins, they seem to form, however, a comparable biomass (Sieburth, 1983; Sherr *et al.,* 1986; Geider, 1988). As far as we know, their optical properties have not been determined and their possible impact upon the optical properties of oceanic waters remains unknown, thus the present study aims at filling this gap. It is an extension of the previous work concerning bacterioplankton, carried out with the same motivations.

Albeit unwanted, heterotrophic flagellates and, to a lesser extent, ciliates were regularly observed in (and eliminated from) bacterial cultures. By modifying the screening protocols and using freshly prepared bacterial suspensions as food, flagellates and naked ciliates were separately grown. The suspensions were then concentrated in view of performing the optical measurements. Among common problems inherent to this kind of culture, one is specifically linked to the optical experiments envisaged here, namely the need for obtaining and selecting a population well defined, if possible, by a narrow size distribution function (regardless of taxonomy). It is a prerequisite for a meaningful interpretation of the optical measurements and their transcription in terms of scattering and absorption efficiency cross sections, a prerequisite which entails some difficulties, in particular a loss of material during the purification, sometimes prejudicial to the pursuit of the experiment.

The present paper is arranged in a fashion similar to that previously adopted when reporting on bacteria, but it is somewhat abridged to avoid useless redundancy. The theoretical approach, as developed for algal cells (Morel and Bricaud, 1986), remains entirely valid for the less pigmented protozoa. The simplified expressions, the derivation of which was possible for bacteria because of their small size (Morel and Ahn, 1990), have to be abandoned and replaced by the general expressions, when dealing with these larger protists.

The optical role of these heterotrophic nanoplankton is also compared to that of bacterio-plankton previously discussed (Morel and Ahn, 1990). Then, the cumulated effect of the whole heterotrophic compartment (bacteria, flagellates and naked ciliates) is tentatively assessed and compared to that of the phototrophic compartment in view of understanding the formation of the optical properties of ocean Case 1 waters. Such an attempt presently comes up against several difficulties, as the rather sparse information concerning the relative numerical abundance of the various heterotrophs in open ocean or also the fact that the species here studied are not exhaustively representative of all existing populations. It is however believed that

this exercise is timely at least as being able to provide working hypotheses for future works.

2. Material and methods

a. Preparation and culture of heterotrophic flagellates and ciliates. Flagellates were grown by using free-living bacteria as food according to a method derived from those described in Fenchel (1982) and Rivier *et al.* (1985). In a preliminary stage, bacterial cultures were grown to final concentrations of about 10^8 cell ml^{-1} in slightly supplemented media, as described in Morel and Ahn (1990). Flagellates were isolated from sea water, (sampled at 10 meters, off Villefranche sur mer) by gravity filtration onto Nuclepore filters with a 5 μm pore size. A volume of 10 ml of this filtrate, used as inoculum, is added to 50 ml of pure bacteria culture. After 2–3 days (in darkness at $18 \pm 1°C$), the culture is passed through a sieve (Nitex, 10 μm) to remove detritic particles and also those ciliates which often have simultaneously grown; 50 ml of fresh bacterial culture is then added. During the following 3 or 4 days, flagellates are fed by daily addition of bacteria. After the last addition, the culture is left for one day, that allows the clearance for bacteria to be largely effected by flagellates. A filtration through a 7 μm Nitex screen again eliminates the larger particles. In view of increasing the flagellates concentration (in particular with respect to that of the remnant bacteria), the culture (about 250 ml) is partly filtered by gravity, under a gentle stirring, onto a 2 μm Nuclepore and thus the volume is reduced to 50–100 ml. The final cell number density amounts to 1–1.5 10^6 cell ml^{-1}, and the population of flagellates, with sizes of *ca.* 3 μm, is (from an optical viewpoint; see below) free from other interfering particles, like remnant bacteria.

Ciliates were isolated and then cultured in a similar way, but Nitex, with 20 μm pore size, is used to prepare the inoculum. During the growing phase with bacterial food addition, flagellates also develop and are submitted to grazing by ciliates. At the end, the ciliates suspensions are purified by two successive filtrations first onto 20 μm Nitex and then 7 μm Nitex screens. The second filtration results in an increase of the ciliates concentration by a factor of about 5, and in the removal of most of the small particles (bacteria, flagellates and small debris). The presence of detritus or dead cells, with sizes in the range of those of ciliates (~11–18 μm) cannot be avoided. Before pursuing any measurement, it is necessary to check (by microscopic examination) if these unwanted particles have remained under a low and acceptable level. Several experiments were left out at this stage, because this condition was not fulfilled. Besides being delicate, these organisms tend to assemble and to adhere onto filters and walls, with the consequence of reducing the available biovolume and cell concentration with respect to what could be expected at the start of the growing experiments. Final concentrations of pure ciliates were about 5 10^4 cell ml^{-1} in successful experiments.

b. Cell enumeration and size distribution. A Coulter Counter ZBI is used to determine the cell number density, N/V. The results, averaged over 10 determinations, coincide well (within better than 5%) with simultaneous microscopic enumeration. The cell size distribution function, $F_r(d)$ is determined in relative values by using a 100-channel analyzer (model C 1000) operated with a 50 μm aperture tube. This function is then transformed into absolute values $F(d)$, by demanding that the integrated value of $F_r(d)$ be equal to the actual number density N/V as previously determined. The determinations of $F_r(d)$ must be carried out when the cells are alive, because it has been observed that any addition of buffered formaline, even at low concentration (0.2%), provokes a detectable reduction in size (Putt and Stoecker, 1989; see also results). Such a bias would preclude any confidence in the optical properties interpretation (or in the carbon-biovolume relationship), which both require a precise determination of $F_r(d)$. This need for keeping the cells alive when determining their size distribution of their optical properties is troublesome, particularly in the case of the sensitive ciliates. Ultra-clean, well polished optical cuvettes do not "attract" living ciliates, at least for the duration of measurements if done quickly. Note that for numerical density N/V measurements, it is easier, and in effect it is necessary, to kill the cells with formaline.

c. Optical coefficients. The method (Bricaud *et al.,* 1983) developed for the determination of the absorption and attenuation coefficients by algal cells, $a(\lambda)$ and $c(\lambda)$ respectively, can be used without change when dealing with heterotrophic organisms in suspension. The measurements, between 400 and 750 nm, were successively carried out by using a Perkin-Elmer 571 spectrophotometer equipped with the scattered transmission accessory and cuvettes close to the detector (absorption configuration), or by setting up the cuvettes far from it (attenuation configuration). With respect to the arrangement described in Bricaud *et al.* (1983), the acceptance angle in the later configuration was reduced from 0.25° down to 0.12° with appropriate diaphragms. The forward scattered radiation still entering the detector has been estimated (via Mie computations) and amounts to about 1.4% and 0.3% of the total scattering coefficient, $b(\lambda)$, in the case of ciliates and flagellates respectively. Therefore the coefficient, as actually determined in the attenuation configuration, can be safely considered as being $c(\lambda)$ without any correction. Then $b(\lambda)$ is obtained as the difference

$$b(\lambda) = c(\lambda) - a(\lambda).$$

The remnant bacteria cannot bias the absorption and scattering values to be measured for bigger organisms. The absorption and scattering cross sections of microbes are smaller by more than 3 (4) orders of magnitude than those of flagellates (ciliates) (see later, Table 2). Even with the measured residual concentration of 10^6 cell ml^{-1}, the bacterial contributions to the absorption and scattering values remain below 1%.

The absorption spectra were also determined below 400 nm (actually from 350 and up to 750 nm), after the organisms have been collected onto GF/F Whatman disks maintained wet for the measurement. The corresponding coefficients, not corrected for the unknown amplification resulting from the diffuse lighting condition, are to be considered only in relative units. Nevertheless, they can provide useful information in the near-UV domain.

The attempts for measuring the backscattering coefficient, according to the method developed when studying bacteria, were unsuccessful, because of the weakness of the signal to be detected.

d. Carbon-nitrogen composition. Known numbers of flagellates were collected by filtration onto pre-combusted GF/F filters and kept frozen until analyzes. The C and N determinations were carried out by using a C-H-N Elemental Analyzer calibrated with glycocol. The biovolume being known, the intracellular carbon concentration $c_{i,c}$ (kg m^{-3}) can be computed, as well as the C-to-N ratio (mass per mass). For ciliates, the C-N determinations failed or were unreliable, mainly because the amount of "pure" ciliates on the filter was insufficient.

3. Results

a. Size distribution functions. The heterotrophic nanoflagellates collected at various dates (between December 1988 and August 1989) and then cultivated do not significantly differ in size (Fig. 1a). The relative distribution functions, normalized by their maximum, are relatively narrow with a peak occurring within the 2.8–3.2 μm interval. Microscopic examination showed that spherically shaped cells are largely predominant. Before the 7 μm screening, examinations and counting demonstrated the presence of some other larger and less regularly shaped flagellates, in the size range 6–8 μm. The biovolume corresponding to these larger protists was always well below that corresponding to the population selected by the 7 μm sieving. Thus the optical experiments were restricted to this "pure," supposedly monoxenic, population of 3 μm-flagellates (likely *Pseudobodo* sp., as in the experiment reported by Rivier *et al.,* 1985).

In Figure 1b are displayed the size distribution functions obtained with cultured aloricate ovoid ciliates (*Uronema* sp.; Rassoulzadegan, personal communication). In one occasion the function was found bimodal with the major peak at about 18 μm and a second one at 13 μm. The other successful cultures revealed Gaussian distributions centered at 13.5 μm, presumably attributable to a monospecific population. The optical measurements were carried out only with the two unimodal populations (See Table 1).

The above mentioned reduction in size subsequent to formaline addition is almost instantaneous; it has been verified that this reduction is not artificial (i.e., due to a change in conductivity). The shifts of the $F_r(d)$ distributions, immediately after
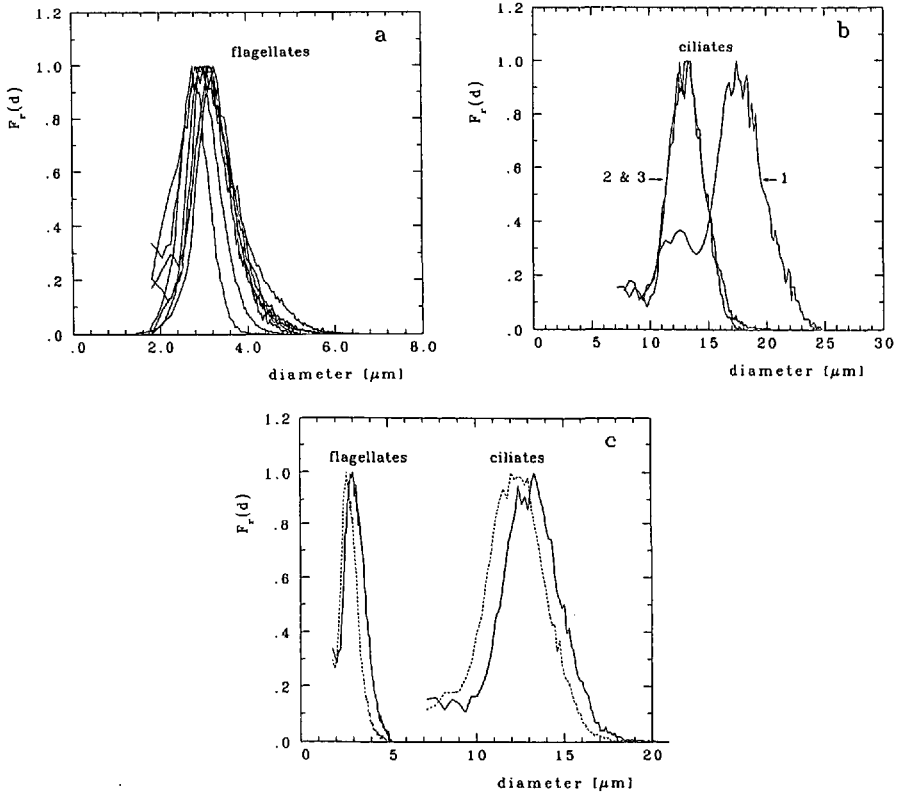
Figure 1. Relative distribution function $F_r(d)$, normalized by their maximum, determined for flagellates and ciliates populations grown in culture (panels a and b, respectively). Shift toward smaller sizes observed for both ciliates and flagellates, instantaneously after formalin treatment; $F_r(d)$——before, and······just after addition (panel c).

addition and shaking, are shown on Figure 1c. The corresponding changes in volume are -25% and -18% for flagellates and ciliates respectively; higher figures (-30% and even -50%) have been observed after several hours.

b. Optical efficiency factors. The dimensionless efficiency factors for absorption and scattering, $\overline{Q}_a$ and $\overline{Q}_b$ (i.e., the ratios of radiant energy absorbed within, or scattered by, the cell, to that impinging onto its geometrical cross-section) and their sum $\overline{Q}_c = \overline{Q}_a + \overline{Q}_b$, are computed in reference to a "mean" cell (i.e., the cell which would have a geometrical cross section equal to the mean of the cross sections of the whole population); therefore these $\overline{Q}$ factors are computed according to

$$\overline{Q}_j(\lambda) = j(\lambda) \left(\pi/4 \int_0^\infty F(d) \, d^2 dd\right)^{-1} \tag{1}$$

where j is either a or b or c. The $\overline{Q}_a(\lambda)$ spectra for both heterotrophic organisms are presented in Figure 2a. Their shapes, with a distinct maximum at about 410–415 nm

Table 1. Relevant information concerning the flagellates (F) and ciliates (C) culture experiments and the optical or chemical determinations.

Experiments	d_1 [μm]	Δd [μm]	d_2^* [μm]	d_3^* [μm]	c, a†	a_f	$c_{i,C}$ [kg m^{-3}]	C/N [g/g]
F-1	—	—	—	—	—	x	—	—
F-2	3.01	0.83	3.19	3.22	x	x	123.4	4.53
F-3	3.11	0.98	3.40	3.44	x	—	134.5	4.83
F-4	3.20	1.01	3.37	3.42	x	—	—	—
F-5	3.01	1.31	3.37	3.42	x	x	126.3	5.04
F-6	3.06	1.56	3.58	3.67	x	—	139.5	4.95
F-7	3.16	1.02	3.62	3.67	—	x	119.3	4.76
F-8	3.25	0.97	3.52	3.58	x	—	144.5	5.24
F-9	2.81	0.75	2.90	2.92	—	x	115.2	5.70
C-1	12.9:17.8	4.26	17.9	18.1	—	x	—	—
C-2	13.5	3.45	13.5	13.7	x	x	—	—
C-3	13.2	3.44	13.4	13.5	x	—	—	—
Averages (±σ)							129 ± 10	5.01 ± 0.35

Meaning of symbols:

d_1 is the modal diameter (2 values are given when the size distribution is doubly peaked).

Δd: width of size distribution (with $F_r(d) > 0.5$).

*: mean diameters, d_2 and d_3, of sphere having a geometrical cross section, or a volume, equal to the average cross section, or to the average volume, of the population, respectively; (see Eq. 17a and 17b in Morel and Ahn, 1990).

†: c, a: respectively attenuation and absorption measurements on flagellates and ciliates in suspension. (x) and (—): determinations made or not made.

a_f: absorption measurement on cells when collected onto GF/F filter.

$c_{i,C}$: intracellular carbon concentration; C/N: carbon-to-nitrogen ratio.

and decreasing values toward the red end of the spectrum, are very similar to that observed for free living bacteria (Fig. 3a in Morel and Ahn, 1990). Their magnitudes, however, are notably different; in comparison with microbes, $\overline{Q}_a$ is largely increased, by about 2–4 fold for flagellates or by 10 fold for ciliates. The cytochrome signature (the Soret band at 415 nm) is well expressed by absorption measurements, extended down to 350 nm, as performed when organisms are collected onto wet GF/F filter (Fig. 2b), instead of being in suspension. Flagellates, and more particularly ciliates, exhibit a stronger absorption in the UV part than do bacteria and the minimum at 385 nm is less accentuated. It cannot be excluded that the smoothing of the minimum may originate from the inevitable presence of detritus (in the ciliates culture especially). The other weak cytochrome bands (*ca.* 525 and 555 nm) are also detectable.

As for bacteria, extractions by acetone and by methanol have been attempted according to the Kishino *et al.* method (1985). The yield of extraction remains poor and the pigmentation of these cells is only weakly reduced. The absorption spectra of the extracts (Fig. 2c) have much in common with the spectra obtained for bacteria,
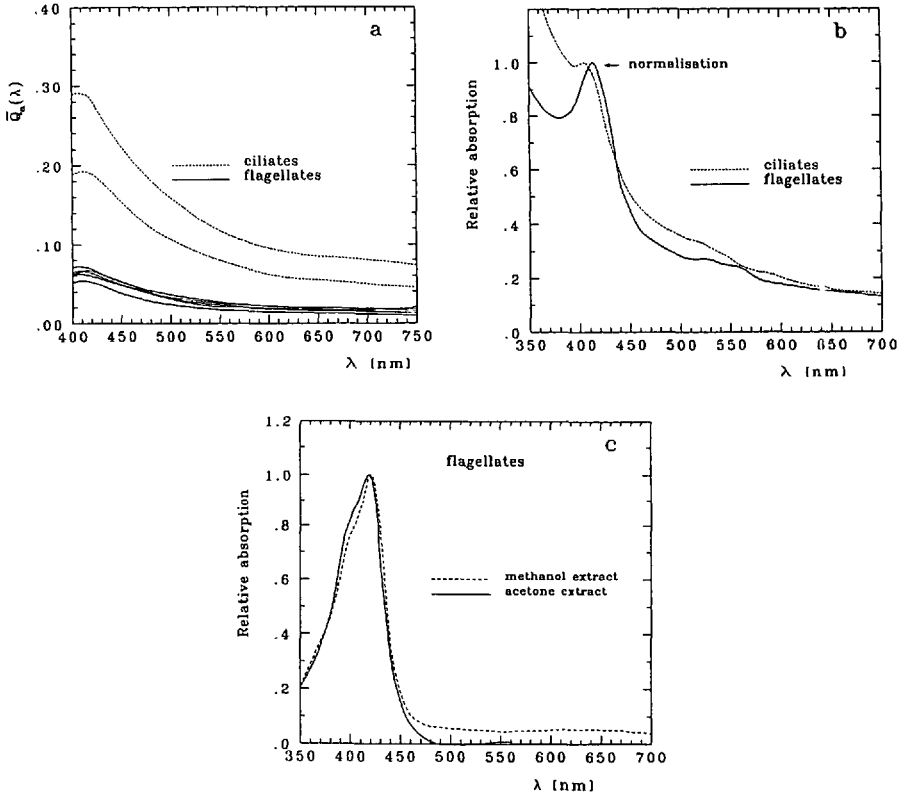
Figure 2. (a) Efficiency factor for absorption as function of wavelength for ciliates and flagellates. (b) Spectral absorption values, normalized by their maximum near 415 nm, when measurements are carried out with cells collected onto a GF/F; (c) absorption spectra (normalized as above) of acetonic and methanol extracts for flagellates only.

apart from the spectacular deepening of the minimum in the UV domain and also from the fact that the maxima in acetone and in methanol, (which were found separated in the case of bacteria) are here coincident.

The absorption spectra of living heterotrophs (including bacteria, as shown in Morel and Ahn, 1990) are very similar to the absorption spectra attributed to bio-detritus as derived from field experiments by using a variety of methods (see e.g. Kishino *et al.,* 1985; Roesler *et al.,* 1989; Morrow *et al.,* 1989; Bricaud and Stramski, 1990). Their common feature is the ascending slope toward the short wavelengths domain and it can reasonably be conjectured that part of this nonalgal absorption originates from the presence of small heterotrophs retained on the filters. Actually the peak at 415 nm, typical of these organisms, is detectable in some "bio-detrital spectra," particularly when measurements are extended down to 350 nm (Kishino *et al.,* 1985) or 380 nm (Bricaud and Stramski, 1990). Its relative prominence, however, is strongly reduced with respect to that of "pure" heterotrophs. The partial contribu-
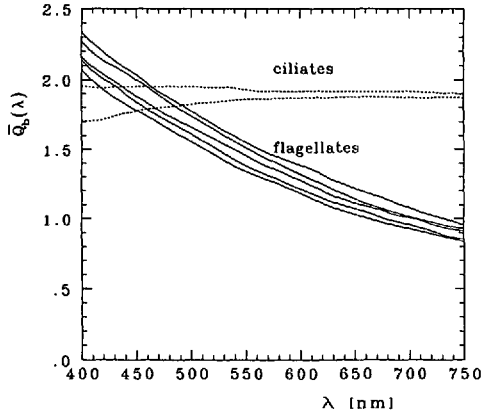
Figure 3. Efficiency factor for scattering as a function of the wavelength for flagellates and ciliates (all experiments).

tion of these organisms, compared to that of other blue absorbing particles, remains presently difficult to quantify. The micro-spectrophotometric technique developed by Iturriaga *et al.* (1988) and Iturriaga and Siegel (1989), which allows the absorption cross section for an individual cell or for any other identified particle to be determined, could help in this problem. To the extent that in natural environment (and conversely to the present experiments) ciliates and flagellates feed also on small phytoplankton and cyanobacteria, they likely keep the signature of photosynthetic, active or degraded, pigments.

In Figure 3 are displayed the $\overline{Q}_b$ (λ) spectra for both populations. The regular concave shape, with increasing values toward the short wavelengths is a common pattern of small scattering bodies such as flagellates. The curvature is well described by a $\lambda^{-1.45}$ dependency, instead of a strict λ^{-2} dependency, as theoretically expected for smaller particles and actually observed with bacteria (Morel and Ahn, 1990). At 400 nm flagellates are able to scatter about twice the amount of radiation they geometrically would intercept, a higher figure than those determined for small sized (1.15–1.5 μm) cyanobacteria, which exhibit $Q_b(400)$ values in the range 0.7–1 (Bricaud *et al.*, 1988: Stramski and Morel, 1990), or those determined for heterotrophic bacteria (0.7 μm), with $\overline{Q}_b(400) \simeq 0.3 - 0.6$ (Morel and Ahn, 1990). The ciliates exhibit a rather flat $Q_b(\lambda)$ curve. The decreasing trend in the blue-violet part of the spectrum is essentially a response to increasing absorption (Fig. 2a) in such a way that the attenuation factor $\overline{Q}_c (= \overline{Q}_a + \overline{Q}_b)$ remains close to 2, whatever the wavelength. This figure is typical of particles rather large compared to the wavelength.

c. Elemental composition. The carbon concentration within the cellular material of flagellates is practically constant (within $\pm$ 8% at 1σ), with a mean value of 129 kg C

m^{-3}, higher than the value (100 kg C m^{-3}) given by Børsheim and Bratbak (1987) but distinctively lower than that determined for bacteria (228 kg C m^{-3}; see in Morel and Ahn, 1990). The relative proportion of proteins also appears slightly lower, as the mean C/N ratio is about 5 (± 0.35 at 1 σ), instead of 4.46 (± 0.71) for microbes.

4. Interpretation

a. Absorption by the cellular material. The absorption coefficient of the cellular material, $a_{cm}(\lambda)$, in m^{-1}, can be derived from the $\overline{Q}_a(\lambda)$ values previously presented, by using the iterative method as developed by Bricaud and Morel (1986), and subsequently modified by Stramski *et al.* (1988). In essence (details to be found in the above references), the iterative scheme is as follows. The Q_a values are theoretically depending on a dimensionless parameter ρ', itself depending on the imaginary part of the index of refraction of the matter forming the cells, n', and on the size parameter α, according to the following relationships and definitions

$$n'(\lambda) = \lambda \, a_{cm}(\lambda)/4\pi \, n_w \tag{2}$$

$$\alpha(\lambda) = \pi \, d \, n_w/\lambda \tag{3}$$

$$\rho'(\lambda) = 4 \, \alpha \, n' \, (= a_{cm}(\lambda) \, d) \tag{4}$$

where n_w ($=1.34$) is the refractive index of the surrounding medium (water), d is the diameter of the particle and $a_{cm}(\lambda)$ is the absorption coefficient of the cellular material. Finally the efficiency factor for absorption, Q_a, expressed as (see e.g. Van de Hulst, 1957)

$$Q_a(\rho') = 1 + 2\,\frac{\exp(-\rho')}{\rho'} + 2\,\frac{\exp(-\rho') - 1}{\rho'^2} \tag{5}$$

is a monotonous function of ρ' and increases from 0 to 1, when ρ' varies from 0 to ∞. To account for the fact that the cells are not uniformly distributed in size, a mean factor, $\overline{Q}_a$, of the "mean" cell of the population in question is defined according to

$$\overline{Q}_a(\rho') = \left(\int_0^\infty F(\rho') \, \rho'^2 \, d\rho'\right)^{-1} \int_0^\infty Q_a(\rho') \, F(\rho') \, \rho'^2 \, d\rho' \tag{6}$$

where $F(d)$, the actual size distribution function, is replaced by $F(\rho')$. This substitution would require the knowledge of a_{cm} (or n'; see Eq. 4 above), which precisely is the parameter to be determined. Therefore at each wavelength λ, the $\overline{Q}_a(\rho')$ value, initially computed with an arbitrary value given to n', is iteratively forced to equate the measured factor $\overline{Q}_a(\lambda)$ by varying n', the only one free parameter. When the coincidence is reached, n' is unambiguously determined because of the monotonous character of the $Q_a(\rho')$ function. The same computation, repeated for each λ, produces the $n'(\lambda)$ and the $a_{cm}(\lambda)$ spectra.
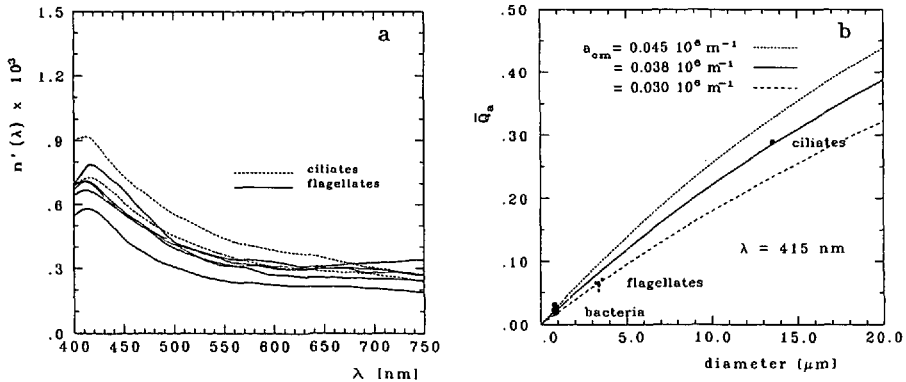
Figure 4. (a) Spectral values of the imaginary part of the index of refraction. (b) Efficiency factor for absorption at $\lambda = 415$ nm for ciliates, flagellates and bacteria as function of their mean diameters; the theoretical curves are computed (Eq. 5) with various values of the absorption coefficient by the cellular material, a_{cm}, as indicated.

The spectral values $n'(\lambda)$ for ciliates and flagellates, shown in Figure 4a, are extremely low, between 2 and 9 10^{-4}, and lower than those computed for free living bacteria. At the wavelength of maximal absorption (415 nm), the absorption coefficients a_{cm} as derived from Eq. 2, are about 0.30 and 0.38 10^5 m^{-1}, for flagellates and ciliates respectively. With these values, pertinent to the cellular material, the $\overline{Q}_a$ (415) values can be computed (Eq. 5 above) as a function of the size of spheres made of these materials (the curves in Fig. 4b). The data for ciliates and flagellates, and in addition those for bacteria, are plotted on the same figure.

b. Scattering efficiency and real part of the refractive index $n(\lambda)$. With n' (λ) determined as said above, the Van de Hulst equation (see Eq. 20 and details in Morel and Ahn, 1990) is iteratively used at each wavelength in order to force the computed $\overline{Q}_c$ (λ) values to reproduce the experimental values and thus to determine n as soon as coincidence is achieved. As discussed in Bricaud and Morel (1986), if $\overline{Q}_c$ (λ) is essentially constant throughout the spectrum (and in that case, is close to 2), the problem remains undetermined, except that a lower limit can nonetheless be assigned to the refractive index. Such a situation is encountered with ciliates; according to their size, n has to be higher than 1.044 to ensure the flatness of the $\overline{Q}_c$ spectrum. On the contrary, the full computational scheme can successfully apply when dealing with flagellates, since $\overline{Q}_c(\lambda)$ (= $\overline{Q}_a(\lambda)$ + $\overline{Q}_b(\lambda)$ separately shown in Figures 2a and 3) is featured with a regular slope toward the blue end of the spectrum.

The n (λ) values computed for flagellates are slightly different from one experiment to another one; they, however, are practically insensitive to the wavelength and the spectra (Fig. 5a) are flat, within ± 0.001. The different values obtained at λ = 415 nm are displayed on Figure 5b as a function of the intracellular carbon
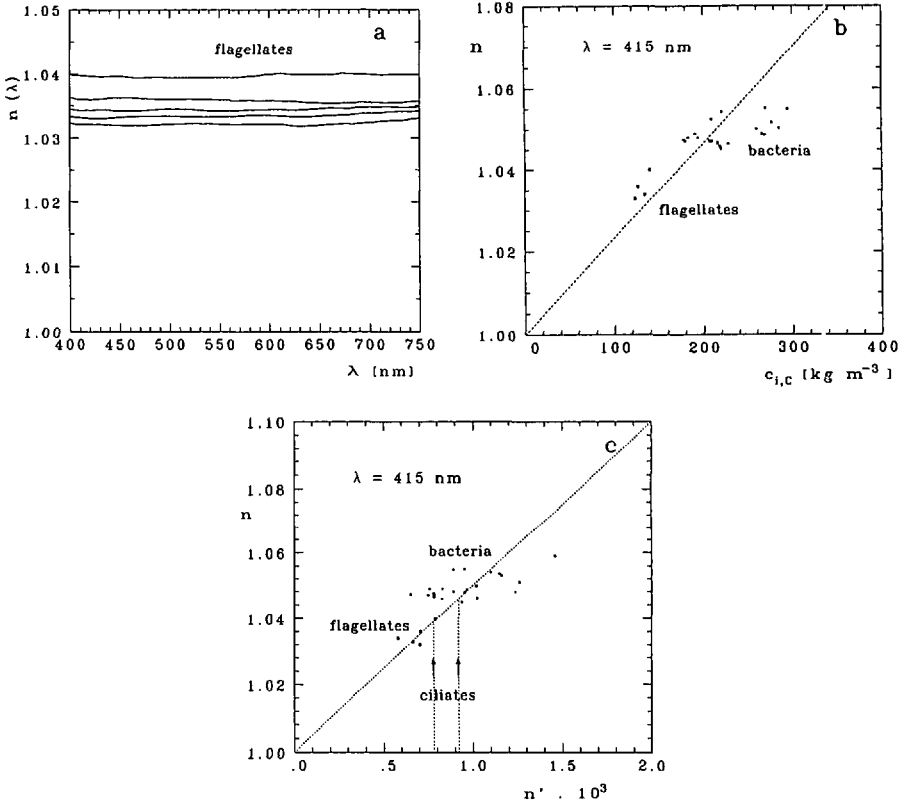
Figure 5. (a) Spectral values of the real part of the index of refraction for flagellates. (b) Index
of refraction (real part) at $\lambda = 415$ nm of flagellates and bacteria (Morel and Ahn, 1990)
plotted as function of intracellular carbon concentration; (c) real part vs imaginary part of
the refractive index for bacteria and flagellates; the two arrows delimits the range of the n'
values obtained for ciliates.

concentration. They are distinctly lower than those computed for free living bacteria,
in agreement with the prediction of a linear relationship between the refractive index
and $c_{i,C}$ according to

$$n = 1 + 0.233 \ 10^{-3} \ c_{i,C}. \tag{7}$$

This relationship, proposed in Morel and Ahn (1990), is shown as the dashed line in
Figure 5b. Unfortunately the unreliability of the $c_{i,C}$ determination for ciliates
prevents one from using Eq. 7 to infer their index n, which also was not derivable
from the optical parameters.

Another approach can be attempted. To the extent that for these heterotrophic
organisms (bacteria, flagellates and ciliates), the absorbing substance at 415 nm
(mainly the respiratory pigments) would be a constant fraction of the carbon content,
there would exist a linear relationship between n' and n. This constancy is roughly
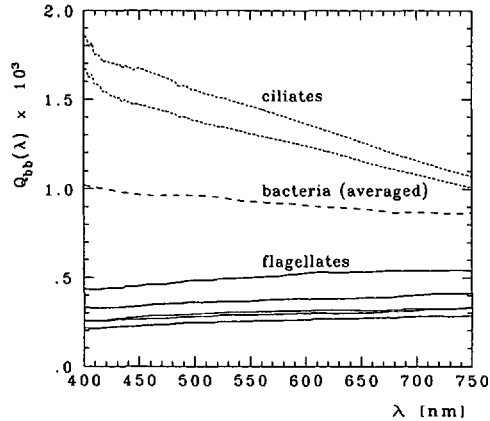
Figure 6. Spectral values of the efficiency factors for backscattering as computed for flagellates and ciliates (see text), or averaged from experimental data in the case of bacteria (Morel and Ahn, 1990).

confirmed by the data for bacteria and flagellates as shown in Figure 5c and can be tentatively used for ciliates. The imaginary part of the index, n', determined for ciliates (Fig. 4a) when transferred into Figure 5c, would lead to n values within the approximate range $1.040 - 1.045$, intermediate between those measured for flagellates and bacteria (and under proviso that the above assumption holds true). This value is compatible with the lower limit 1.044 previously found; note that by inverting Eq. 7 and using these tentative n values (between 1.040 and 1.045), it would result $c_{i,C}$ values for ciliates within the range 172–193 kg C m^{-3}.

c. Backscattering efficiency. In absence of direct determination of the backscattering coefficient, the backscattering efficiency $\overline{Q}_{bb}$ can be computed through the use of the Mie theory. $\overline{Q}_{bb}$ is that part of $\overline{Q}_b$ which corresponds to backscattered radiant energy only (also defined in reference to the energy impinging onto the geometrical cross section of the particle). With the spectral values $n(\lambda)$ and $n'(\lambda)$, combined with the size distribution function $F(d)$, the Mie code is operated and produces the volume scattering function $\beta(\theta)$ for each wavelength (with $\Delta\lambda = 2.5$ nm between 400 and 750 nm). The ratio of the integral of these functions over the backward directions $(\pi > \theta > \pi/2)$ to the integral over the whole angular domain $(\pi - 0)$ provides $\overline{Q}_{bb}(\lambda)$ (see also Eq. 11). The results of these computations are shown on Figure 6. The needed information being complete for flagellates, the spectra for all cultivated populations are computed and displayed, whereas the computation is effected after having adopted the same constant n value (1.044) for the two ciliates populations.

Flagellates have a featureless backscattering spectrum with an efficiency lower than that of free living bacteria. On the contrary ciliates exhibit increased $\overline{Q}_{bb}$ values in the blue with higher values than microbes everywhere in the spectrum (still rather

weak, however). This nonmonotonic behavior of Q_{bb} with respect to size (a minimum for flagellates) and the occasional spectral dependency (for size range corresponding to ciliates) were, in effect, theoretically expected, as shown in Morel and Bricaud (1981).

5. Discussion and conclusions

Optics of the heterotrophic organisms investigated in this paper is well understood in the frame of the anomalous diffraction approximation (Van de Hulst, 1957). For these protists (and also for free living bacteria previously studied in Morel and Ahn, 1990), the optical efficiency factors and their spectral variations conform to the theoretical predictions. Therefore the diffraction approximation and the more general Mie theory can be used to predict other parameters that were not determined (such as the backscattering efficiency) or also to infer the optical behavior of similar protists of other (intermediate) sizes in so far as their cellular material does not dramatically differ from that of organisms already studied. For those studied, the common characteristics are a weak absorption capability (except the discernible maximum around 415 nm) which is related to the presence of respiratory pigments, and a refractive index within the range 1.035–1.045 in relation to the carbon content. In comparison, heterotrophic bacteria as well as cyanobacteria (see in Stramski and Morel, 1990) are slightly more compact and refringent, or equivalently less watery, bodies than larger heterotrophs. This trend is confirmed by recent observations which demonstrate that diminutive bacteria have a high dry matter-to-volume ratio (Norland *et al.,* 1987; Simon and Azam, 1989). In conclusion, even at the wavelength where they are more absorbing (415 nm), all these heterotrophic oganisms act essentially as scatterers, and the Q_b-to-Q_a ratios quantify this dominance (see values in Table 2). For this reason the following discussion will be restricted to their possible role in the light scattering process within oceanic waters.

a. Contribution of heterotrophic bacteria and nanoplankton to the scattering by oceanic waters. It has been possible to empirically relate the optical properties of oceanic Case 1 waters (in the euphotic zone) to their chlorophyllous pigment concentrations, and in particular, the scattering coefficient at $\lambda = 550$ nm, b in m^{-1}, has been found to be nonlinearly dependent on the (chlorophyll + pheophytin) concentration, $\langle$chl$\rangle$, in mg m^{-3}, according to (Gordon and Morel, 1983)

$$b = 0.30 \ (\pm \ 0.15) \ \langle \text{chl} \rangle^{0.62}. \tag{8}$$

The backscattering coefficient, b_b, at 550 nm, is also empirically related to $\langle$chl$\rangle$ through (Morel, 1988)

$$b_b = b \ [2 \ 10^{-3} + 2 \ 10^{-2} \ (\tfrac{1}{2} - \tfrac{1}{4} \log_{10} \langle \text{chl} \rangle)] \tag{9}$$

where b comes from Eq. 8.

Table 2. Geometrical cross section (s), refractive (real) index of refraction n, mean optical efficiency factor (Q) and optical influences of flagellates and ciliates compared to those of bacterioplankton (uniform population of "reference" cells, see text). In the columns "Σ," values of the cumulated (bacteria + flagellates + ciliates) contributions, in reference to that of the sole bacterioplankton compartment.

	bact.1	flag.1	cil.1	$\Sigma 1$	bact.2	flag.2	cil.2†	$\Sigma 2$
d (as 10^{-6} m)	0.55	3.4	13.5		0.66	5.0	13.5	
n	1.05	1.04	1.04		1.05	1.04	1.04	
s (as 10^{-12} m^2)	0.24	9.08	143		0.33	19.6	143	
Mean $Q_a(415)$	0.0150	0.06	0.24					
(550)	0.0035	0.02	0.10		0§	0	0	
Mean $Q_b(415)$	0.1556	2.15	1.85					
(550)	0.0886	1.60	2.00		0.124	2.85	2.0	
Mean $Q_{bb}(550)$	0.0010	0.0006	0.0011		0.0009	0.0006	0.0011	
$\overline{Q_a}/\overline{Q_b}$								
at 415 nm	9.6%	2.8%	13%					
550 nm	4%	1.3%	5%					
Relative numerical abundance								
	1	$1/10^3$	$1/10^5$		1	$1/10^3$	$1/10^5$	
Relative biomass								
	1	0.24	0.15	1.40	1	0.46	0.09	1.55
Relative total scattering coefficient								
at 415 nm	1	0.53	0.07	1.60				
550 nm	1	0.69	0.14	1.83	1*	1.37	0.07	2.44
Relative backscattering coefficient								
at 550 nm	1	0.0230	0.0066	1.03	1	0.04	0.005	1.045

†cil.2 does not differ from cil.1.

§For bact.2, flag.2 and cil.2, the imaginary part of index (at 550 nm) is set equal to zero and thus $Q_a(550) \equiv 0$.

*Note that the scattering coefficient of bact.2 is twice that of bact.1.

Assessing the contribution of the heterotrophic organisms to the bulk optical properties of the upper layer of the ocean requires information about the size distribution and numerical abundance of these organisms, preferably in relation to the algal pigment concentration, in view of comparison with the values produced by Eq. 8 or 9, which depend on $\langle$chl$\rangle$.

The first attempts in this direction were restricted to the sole heterotrophic bacterioplankton compartment, the estimation of its optical contribution took advantage of the existence of relationship between bacterial abundance and Chl-*a* concentration. Namely the relationship proposed by Cole *et al.* (1988) was used by Morel and Ahn (1990) and that displayed in Cho and Azam (1990) was used by Stramski and Kiefer (1990). Recent data obtained in the oligotrophic eastern Mediterranean Sea (1.8 to 4 10^{11} bacterial cells m^{-3} for water with 0.04 to 0.15 mg chl *a* m^{-3}, according to M. Wood and T. Berman, pers. comm.) and also a review of numerous data prepared by W. K. W. Li (pers. comm.) tend to support the validity of

the Cole *et al.*'s relationship, in particular in oceanic oligotrophic environments; this relation

$$[N/V]_m = 0.91 \ 10^{12} \ \langle \text{chl} \rangle^{0.52} \tag{10}$$

where $[N/V]_m$ is the microbe abundance (cell m^{-3}), is adopted for what follows. To go further and account for all kinds of larger heterotrophs, some assumptions are needed because their abundance is still incompletely documented.

A first approach consists of keeping close to the present optical data obtained for particular organisms (including free living bacteria) and combining them with information found in literature concerning the relative numerical abundances within the heterotrophic compartment. Such an approach obviously is open to criticism to the extent that these organisms which were isolated and investigated in the present study, are in some way treated as "generic" flagellates and ciliates, notwithstanding the rather wide diversity in size and nature which occurs in natural environment. Keeping in mind this caveat, it is believed, however, that a first insight can be gained through such a trial. It can be completed by another approach resting on plausible optical properties for heterotrophic plankton, as derived from theory, then combined with a generalized size distribution function, as originally suggested by Sheldon *et al.* (1972).

b. First approach. Even if information concerning heterotrophic nanoplankton is less systematic than for bacteria, it is nevertheless acknowledged that in open ocean they form a considerable part of the total biomass, perhaps equivalent to that of their phototrophic cousins within the same size range, although smaller than that attributed to the bacterioplankton (see e.g. Azam *et al.,* 1983 and Sieburth, 1983). Many observations (Geider, 1988 and references therein) suggest that flagellate abundances are commonly in the range of 10^8 to 10^9 cells m^{-3}, in other words, smaller than numerical abundance of microbes by about 3 orders of magnitude. According to Sieburth (1983), in offshore water the small (2–5 μm) flagellates would maintain an approximate ratio of 1/1250 in number with respect to bacteria. This figure is fully consistent with numerous observations in the oligotrophic waters of Mediterranean Sea (Rassoulzadegan, pers. comm.). Aloricate ciliates (with equivalent spherical diameters < 20 μm), which may be an important component of the heterotrophic nanoplankton, have been reported in many parts of the ocean (Sherr *et al.,* 1986 and references therein). Ciliate and flagellate biomasses would be within the same order of magnitude leading to numerical abundances in a ratio of about 1:100 (Sherr *et al.,* 1986).

According to these observations, we suggest a ratio of the number of flagellates to that of microbes, $r_{f,m} = 1{:}10^3$ and a ratio of the number of ciliates to that of microbes, $r_{c,m} = 1{:}10^5$. By allowing that on average pelagic bacteria, nano-flagellates and naked ciliates have equivalent sphere diameters $d_m = 0.55$, $d_f = 3.4$ and $d_c = 13.5$ μm

respectively, their optical contributions can be established in reference to those of bacterioplankton (see Table 2 "bact.1, flag.1, cil.1"). The size adopted for bacteria (0.55 μm) is similar to the smallest observed in unenriched culture experiments (0.59 μm, in Morel and Ahn, 1990), and believed to be representative of cells in natural oceanic environment (Ducklow, 1986; Cho and Azam, 1990). The sizes adopted for flagellates and ciliates are those determined for the species presently investigated, and they agree with most of the field observations. If the interspecific cellular carbon concentration $(c_{i,C})$ differences are discarded, the biomasses related to each category simply vary as d^3, i.e. as biovolumes. Therefore under the above assumptions about the numerical abundances, the flagellates biomass would represent 24%, and ciliates biomass 15%, of the bacterial biomass (or biovolume).

With $d_m = 0.55$ μm, $n = 1.05$, $n'(550) = 3 \ 10^{-4}$ and $n'(415) = 10^{-3}$, the adopted "reference" bacterium exhibits the efficiency factors given in the first column of Table 2 (bact.1); Q_b and Q_a have been computed through Eq. 9 and 12 in Morel and Ahn (1990) (with n_w the refractive index of water = 1.34), and Q_{bb} has been derived through

$$Q_{bb} = \left[\int_{\pi/2}^{\pi} \beta(\theta) \ \sin\theta \ d\theta \Big/ \int_{0}^{\pi} \beta(\theta) \ \sin\theta \ d\theta\right] Q_b \tag{11}$$

where $\beta(\theta)$, the volume scattering function, has been computed through Mie theory using the above d_m, n and n' input parameters, and where the ratio of the two integrals represents $\tilde{b}_b$, the backscattering ratio.

The scattering and backscattering coefficients (with subscripts m) resulting from the presence of microbes, with a numerical abundance $[N/V]_m$ expressed according to Eq. 10, and a geometrical cross section s_m ($=0.24 \ 10^{-12}$ m^2), are

$$b_m = [N/V]_m \ s_m \ Q_b = 0.0192 \ \langle\text{chl}\rangle^{0.52} \ (\text{at } \lambda = 550 \text{ nm}) \tag{12}$$

and

$$b_{b,m} = [N/V]_m \ s_m \ Q_{bb} = 2.17 \ 10^{-4} \ \langle\text{chl}\rangle^{0.52} \ (\text{at } \lambda = 550 \text{ nm}) . \tag{13}$$

For flagellates and ciliates, their mean Q_b values given in Table 2 ("flag.1 and cil.1") are adopted from Figure 3 and their Q_{bb} values have been computed by operating the Mie code. Then their contributions to the scattering and backscattering coefficients are obtained as

$$\begin{bmatrix} b_i \\ b_{b,i} \end{bmatrix} = (N/V)_i \ s_i \begin{bmatrix} \overline{Q}_{b,i} \\ \overline{Q}_{bb,i} \end{bmatrix} \tag{14}$$

where the subscript i is either f or c (for flagellates and ciliates) and s is the geometrical cross section. If these contributions are normalized with respect to those
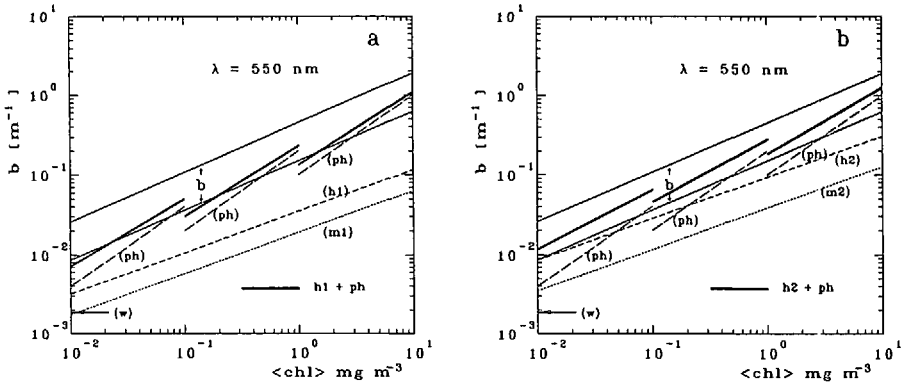
Figure 7. As a function of the chlorophyll concentration, total scattering coefficient for oceanic waters; the stripe denoted "b" corresponds to the extreme values of the coefficient appearing in Eq. 8. In both panels, the lines with "ph" indicate the phytoplankton contributions and the arrows with "w" show the value corresponding to molecular scattering. In panels a and b respectively, the microbial contributions to scattering are identified with symbols m1 and m2 (in reference to the bact.1 and 2 in Table 2) and the all-heterotrophs contributions are identified with the symbols h1 and h2 (see Table 2 and text). The thick lines correspond to the cumulated influences of photo- and heterotrophic organisms ("ph + h").

of the sole microbial compartment, the corresponding ratios are expressed as

$$
\begin{bmatrix} b_i/b_m \\ b_{b_i}/b_{b_m} \end{bmatrix} = r_{i,m} \, (d_i/d_m)^2 \begin{bmatrix} \overline{Q}_{b_i}/\overline{Q}_{b_m} \\ \overline{Q}_{bb_i}/\overline{Q}_{bb_m} \end{bmatrix}.
\tag{15}
$$

Such a presentation in "relative" optical coefficients allows a generalization of the results to be made. In particular, if the hypotheses concerning the flagellates-to-bacteria and the ciliates-to-bacteria abundance ratios prove to be unrealistic and need to be changed, the modified coefficients can be easily obtained by changing the $r_{i,m}$ values.

The variations of the oceanic scattering coefficient at 550 nm along with $\langle chl \rangle$ are displayed in Figure 7a and the stripe (in log–log plot) corresponds to the upper and lower values of the coefficient appearing in Eq. 8. The contribution of microbes to scattering, computed through Eq. 12, is also shown (line "m1" in Fig. 7a) and amounts to about 14% on average (namely to 7 or 20%, according as the coefficient in Eq. 8 is given 0.45 or 0.15). Such a proportion is approximately maintained throughout the chlorophyll concentration range, in as much as the bacterial number and scattering coefficient are both linked to the $\langle chl \rangle$ concentration through non-linear empirical relationships with nearly equal exponents (0.52 and 0.62 respectively). To account for the influence of larger heterotrophic protists, supposedly in constant relative proportions with bacteria, b_m, at 550 nm, has to be increased by a factor 1.79 (see Table 2 column "$\Sigma 1$") to obtain b_h, the contribution to scattering of

the entire heterotrophic compartment. This increase is not considerable and b_h (line "h1" in Fig. 7a) forms a fraction of about 20–25% of the lower oceanic b values.

It is tempting to analyze the formation of the scattering properties of open ocean case 1 waters by considering in addition the contribution of phototrophic organisms. Recently data appeared about the chlorophyll-specific scattering coefficient of algae, b^* in m^2 (mg chl)$^{-1}$ (Davies-Colley *et al.*, 1986; Weidemann and Bannister, 1986; Morel, 1987); they can be used in the present tentative analysis. To compute b_{ph}, the partial scattering coefficient originating from phytoplankton, according to

$$b_{ph} = b^* \langle \text{chl} \rangle \tag{16}$$

The b^* values determined for the pure algae grown in culture are adopted. They are widely scattered (see Table 1 in Morel, 1987) with, however, a trend for small (1–2 μm) species to exhibit high b^* values, between 0.2 and 0.6 m^2 (mg chl)$^{-1}$, instead of 0.1 or even less for large cells. To derive and plot b_{ph} in Figure 7a the tentative b^* values 0.4, 0.2 and 0.1 m^2 (mg chl)$^{-1}$ have been successively used for the oligo-, meso- and eutrophic situations. This choice accounts for the fact that big species, such as diatoms, are believed to dominate in eutrophic waters, whereas picoplanktonic species would prevail in oligotrophic environments. With these values, the contribution of algae in forming the scattering coefficient appears to be dominant relative to that of the heterotrophic compartment. Under the reservations following from the hypotheses needed in such an approach (some of them are debatable and tentatively modified below), it is nevertheless, comforting to notice the general agreement between the recomposed scattering coefficient (the sum of b_{ph} and b_h) and the b values found in the oceanic environment (at least the lowest b values, when the coefficient in Eq. 10 is 0.15). With an average coefficient 0.30 in this equation, the most common scattering values, in effect, are twice the lowest (or the presently recomposed) b values. The difference can originate from local peculiarities in the algal population, from an underestimate of the role of heterotrophs or also from the ignorance of the detrital compartment.

The chlorophyll-specific scattering coefficient for locally dominant algae may be higher than the selected b^* values. It is an avoidable difficulty when adopting "mean" values. This does not exclude that, in parallel, scattering by heterotrophs, very sensitive to size, has been minimized by the somewhat arbitrary choice made above. With a d^4 dependency (Morel and Ahn, 1990), the microbial scattering contribution is, for instance, doubled if the typical diameter is given the value 0.65 μm, instead of 0.55 μm ("bact.2" in Table 2). If now the "mean" size of flagellates ("flag.2" in Table 2) is assumed to be 5 μm instead of 3.4 μm, the scattering cross section (the product sQ_b) is increased by a factor 3.7 ("flag.2" compared to "flag.1" in Table 2). Without changing the size of ciliates, and using these modified values for typical bacteria and flagellates, b_h now approaches the lower b values in oligotrophic waters and would form 50% of the values in eutrophic waters (see Fig. 7b, curve h2). The auto- and
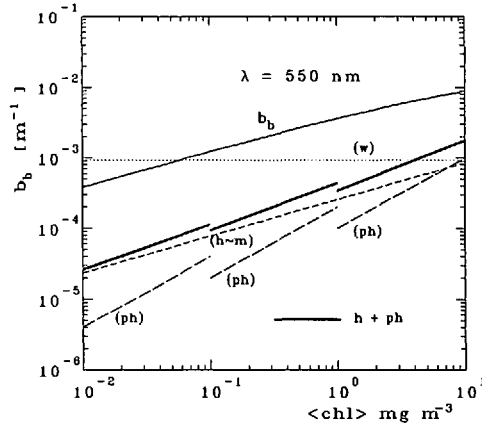
Figure 8. As in Figure 7, but for backscattering; the backscattering coefficient for oceanic waters denoted b_b comes from Eq. 9; the phytoplankton contribution comes from Figure 7 after reduction by 3 orders of magnitude; the backscattering contribution of all heterotrophs is dominated (97%) by that of microbes. The thick lines show the cumulated influences of photo- and heterotrophic organisms ("ph" + "h").

heterotrophs contributions tend to be similar and their addition approximately reproduces the average b values, as derived from Eq. 8, when the coefficient is 0.30. Under these assumptions, the scattering action of bio-detritus and other (not identified) particles would not be decisive, except that their presence in variable amount could be partly at the origin of natural fluctuations, as implicitly acknowledged by the variable coefficient in Eq. 8. Under the previous assumptions (in Fig. 7a) of a reduced influence of heterotrophs on scattering, the role of bio-detritus would have to be reconsidered and heightened. There is presently not enough information to proceed any further and the following conclusions have to be seen as heuristic arguments for future investigations. They could be as follow. The "identified" organisms belonging to the nano- and microplankton compartment play the major role in the scattering process; uncertainties subsist about the respective contributions of photo- and heterotrophic organisms, even if algae seem more efficient, especially in meso- and eutrophic waters; microbes, with typical small sizes as reported, would have only a reduced influence; finally detritus, clearly detected via absorption measurements (see e.g., Kishino *et al.*, 1985 and other references above), could at least contribute to the variability in scattering as observed in natural environment.

In reference now to Eq. 9 and to the backscattering coefficient of oceanic waters, a similar analysis can be undertaken (see Fig. 8). The contribution of microbes to this coefficient is described by Eq. 13 and turns out to be about one order of magnitude below the oceanic values of the backscattering coefficient. According to values given in Table 2, this contribution has to be increased only by 3% to account for all other heterotrophs. In other words, the bigger protists have almost no influence. The role of phototrophic cells can be deduced from the previous b_{ph} values (in Fig. 8) after

multiplying by $\bar{b}_b$, their backscattering ratio. This ratio, theoretically as well as experimentally, proves to be within the $10^{-4}-10^{-3}$ magnitude range (Morel and Bricaud, 1981; Bricaud *et al.*, 1983). Therefore algae (even with $\bar{b}_b$ given its maximum value, i.e. 10^{-3} in Fig. 8) appear to be yet less effective than bacteria in contributing to the formation of the backscattering coefficient. Very small photosynthesizing cyano-bacteria or prochlorophytes could act like heterotrophic bacteria upon backscatter-ing when they are of the same size (leading to increased $\bar{b}_b$ values, of the order of 10^{-2}), but only if their numerical abundance was equivalent. The bulk of algae, however, generally found in the size range of flagellates and ciliates, have almost no influence on b_b.

The final and somewhat surprising result is the very low contribution of "identified" organisms to the oceanic b_b values. Changing the hypotheses about their sizes (as previously done when discussing b) does not significantly alter this conclusion. Unlike b_m, $b_{b,m}$ increases only as d^2 (Morel and Ahn, 1990), therefore the change from 0.55 to 0.65 μm in diameter enhances the microbial contribution by only 40%, that is insignificant with respect to the gap (about one decade) between $b_{b,m}$ and b_b. Even drastically changed, the assumptions relative to the size and abundance of other heterotrophic protists cannot have any palpable effect, because of their very low backscattering efficiency. The missing part, rather considerable, has likely to be attributed to unidentified tiny particles, with presumably large numerical abundance and with high $\bar{b}_b$ ratio, as dictated by their small size (their index has a reduced influence, see Figure 8 in Morel and Bricaud, 1986). This explanation will be supported by other arguments developed below.

c. Second approach. The critical point in the first approach was to consider, and then to add the influences of separate populations with nominal discrete sizes, while it is known that a continuous size spectrum is the rule in the real world. This spectrum is such that, to first approximation, roughly equal concentrations of particulate mate-rial occur in logarithmically equal size ranges (Sheldon *et al.*, 1972; see also discussions in Platt *et al.*, 1984 and in Rodriguez and Mullin, 1986). Such an equipartition implies that the number of particles per size increment dN/dd obeys a Junge distribution (Junge, 1963; Bader, 1970)

$$F(d) = dN/dd = k\, d^{-j} \tag{17}$$

and that $j = 4$; k is a constant related to the absolute number of particles. Actually a slight decrease in biovolumes with increasing sizes is often noticed (see e.g. Rassoul-zadegan and Sheldon, 1986) and this trend would correspond to an exponent value $j > 4$. Superimposed to the general trend, peaks may occur and reveal the dominance of certain species; they cannot be accounted for by the above expression. Detrital particles are included in the size spectrum and no distinction is made between photo- and heterotrophic organisms. This frequency distribution, initially established for
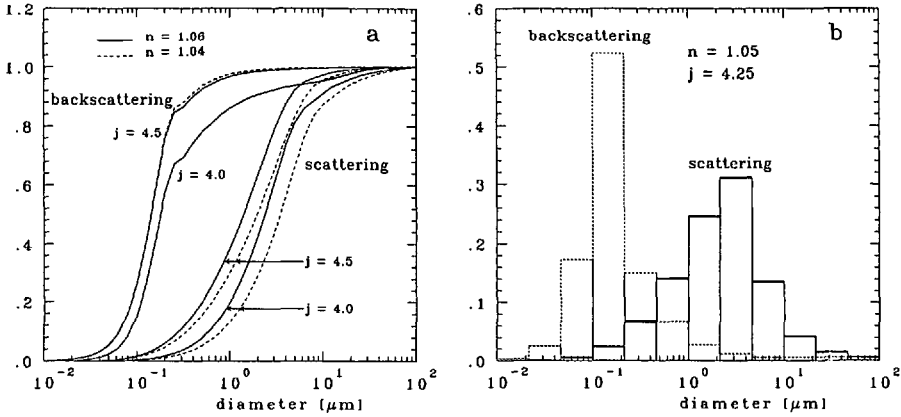
Figure 9. Panel a: Progressive values of the integrals (Eq. 18a and b giving the scattering and backscattering coefficients) when the size increases from 0.01 up to 100 μm, for two values of the relative index of refraction (n) and where the exponent of the (Junge) size distribution (*j*) is given two values, as indicated (Note that when *j* = 4, the backscattering curves for *n* = 1.04 and 1.06 are superimposed). Panel b: by derivation of functions similar to those displayed in panel a, but for *n* = 1.05 and *j* = 4.25, histograms describing the relative contributions of each class of particles (3 per decade) in the formation of the scattering and backscattering coefficients.

size above 1 μm, continues to apply down to the minimum measurable size (about 0.35 μm; Rassoulzadegan and Sheldon, 1986) and encompasses all kinds of organisms, from bacteria, cyanobacteria, hetero- and autotrophic pico- and nanoflagellates, ciliates and microplanktonic algae.

The above continuous size distribution can serve as tool for a closure of the problem addressed. For populations of particles within a size range delimited by a minimal and a maximal value d_{min} and d_{max}, the relative scattering and backscattering coefficients can be computed according to

$$b = \int_{d_{min}}^{d_{max}} F(d) \, s(d) \, Q_b(d) \, dd \tag{18a}$$

$$b_b = \int_{d_{min}}^{d_{max}} F(d) \, s(d) \, Q_{bb}(d) \, dd \tag{18b}$$

where $s(d)$ ($=\pi d^2/4$) is the geometrical cross section and where the efficiency factors Q_b and Q_{bb} are computed through Mie theory as function of the diameter d and the index of refraction (from 1.04 to 1.06). The exponent (*j*) in the distribution function $F(d)$ is given values between 4 and 4.5. The results are presented (Fig. 9a) as the progressive values of the above integrals when the size goes from d_{min} (=0.01 μm) up to d_{max} (=100 μm). The asymptotic behavior of all curves demonstrates that the inclusion of particles above 100 μm will not change the final b or b_b values. An interesting point emerges from this figure; the most efficient contributors to scatter-

ing are particles between, say, 1 and 10 μm (as already shown in Morel, 1973), whereas the dominant particles in the backscattering process are smaller than 1 μm, the most efficient ones being within the 0.1 to 0.4 μm range. This is made clear in Figure 9b where the partial contributions of each size class (to scattering and backscattering) are displayed as function of the size.

Heterotrophic and phototrophic pico- and nanoplankton are just belonging to this size range which provides the effective scatterers. Together with debris of similar size, they could contribute to the scattering coefficient with a weight about 3 to 7 times larger than that of the small fraction <1 μm (depending on n and j). Such relative proportions are in reasonable agreement with those found in the first analysis using discrete sizes and generic organisms.

The missing term in the backscattering process, revealed when the contributions of various identifiable organisms have been added, can now be explained. It suffices that the validity of the Junge distribution, already verified down to ca 0.4 μm, be extended below this limit, at least for the rather restricted range which includes the most efficient backscatterers, i.e. the 0.4–0.1 μm range. Unfortunately these tiny things, at the transition between true particles and colloidal and dissolved pools largely defy characterization, even if they probably form a sizeable part of the oceanic "saprosphere" (Toggweiler, 1990). Just after the submission of the first version of the present paper, it was clearly demonstrated by Koike *et al.* (1990) that candidates for the missing reservoir do actually exist. Non-living, detrital submicrometer particles (95% of these are below 0.6 μm) appear to be much more abundant than bacteria of similar size. With such characteristics and abundance they can play a major role, as yet unsuspected, in the backscattering process. In addition, viruses, in particular those appearing to be free in the water, were recently found to be active members of the microbial food web with numerical abundance exceeding that of bacteria by an order of magnitude (Bergh *et al.,* 1989; Børsheim *et al.,* 1990; Bratbak *et al.,* 1990). Wind-transported minerogenic particles, at least the small size fraction with low settling velocity (Blank *et al.,* 1985), are also potential contributors to the backscattering coefficient, even if unsignificant with respect to the total scattering coefficient.

In summary, the speculative conclusions arrived at when examining the results in Figure 8, then supported on the basis of a simple and plausible assumption (the extension of the same size distribution towards smaller particles than those currently identified and enumerated), begin to receive an experimental confirmation, even if the exact nature and the origins of these numerous tiny particles are still not clear.

REFERENCES

Andersen, P. and T. Fenchel. 1985. Bacterivory by microheterotrophic flagellates in seawater samples. Limnol. Oceanogr., *30,* 198–202.

Azam, F., T. Fenchel, J. G. Field, J. S. Gray, L. A. Meyer-Reil and F. Thingstan. 1983. The ecological role of water-column microbes in the sea. Mar. Ecol. Prog. Ser., *10,* 257–263.

Bader, H. 1970. The hyperbolic distribution of particles size. J. Geophys. Res., *75,* 2822–2830.

Bergh, O., K. Y. Børsheim, G. Bratbak and M. Heldal. 1989. High abundance of viruses found in aquatic environments. Nature, *340,* 467–468.

Blank, M., M. Leinen and J. M. Prospero. 1985. Major asian aeolian input indicated by the mineralogy of aerosols and sediments in the Western North Pacific. Nature, *314,* 83–86.

Børsheim, K. Y. and G. Bratbak. 1987. Cell volume to cell carbon conversion factor for bactivorous *Monas* sp. enriched from sea water. Mar. Ecol. Prog. Ser., *36,* 171–175.

Børsheim, K. Y., G. Bratbak and M. Heldal. 1990. Eumeration and biomass estimation of planktonic bacteria and viruses by transmission electron microscopy. App. Environ. Microbiol., *56,* 352–356.

Bratbak, G., M. Heldal, S. Norland and T. F. Thingstad. 1990. Viruses as partners in spring bloom microbial trophodynamics. App. Environ. Microbiol., *56,* 1400–1405.

Bricaud, A., A. L. Bedhomme and A. Morel. 1988. Optical properties of diverse phytoplanktonic species; experimental results and theoretical interpretation. J. Plank. Res., *10,* N5, 851–873.

Bricaud, A. and A. Morel. 1986. Light attenuation and scattering by phytoplanktonic cells; a theoretical modeling. Appl. Opt., *25,* 571–580.

Bricaud, A., A. Morel and L. Prieur. 1983. Optical efficiency factors of some phytoplankters. Limnol. Oceanogr., *28,* 816–832.

Bricaud, A. and Stramski D. 1990. Spectral absorption coefficients of living phytoplankton and nonalgal biogenous matter. A comparison between the Peru upwelling area and the Sargasso Sea. Limnol. Oceanogr., *35,* 562–582.

Cho, B. C. and F. Azam. 1990. Biogeochemical significance of bacterial biomass in the ocean's euphotic zone. Mar. Ecol. Prog. Ser., *63,* 253–259.

Cole, J. J., S. Findlay and M. L. Pace. 1988. Bacterial production in fresh and saltwater ecosystems; a cross-system overview. Mar. Ecol. Prog. Ser., *43,* 1–10.

Davies-Colley, R. J., R. D. Pridmore and J. E. Hewitt. 1986. Optical properties of some freshwater phytoplankton algae. Hydrobiologia, *133,* 165–178.

Ducklow, H. 1986. Bacterial biomass in warm-core Gulf Stream ring 82-B: mesoscale distribution, temporal changes and production. Deep-Sea Res., *33,* 1789–1812.

Fenchel, T. 1982. Ecology of heterotrophic Microflagellates. I. Some important forms and their functional morphology. Mar. Ecol. Progr. Ser., *8,* 211–223.

Geider, R. J. 1988. Abundance of autotrophic and heterotrophic nanoplankton and size distribution of microbial biomass in the Southwestern North Sea in October 1986. J. Exp. Biol. Ecol., *123,* 127–145.

Gordon, H. R. and A. Morel. 1983. Remote assessment of ocean color for interpretation of satellite visible imagery, a review, *in* Lecture Notes on Coastal and Estuarine Studies, R. T. Barber. C. N. K. Mooers, M. J. Bowman and B. Zeitschel, eds., Springer-Verlag, New York, 114 pp.

Iturriaga, R., B. G. Mitchell and D. A. Kiefer. 1988. Microphotometric analysis of individual particle spectra. Limnol. Oceanogr., *33,* 128–135.

Iturriaga, R. and D. A. Siegel. 1989. Microphotometric characterization of phytoplankton and detrital absorption properties in Sargasso Sea. Limnol. Oceanogr., *34,* 1706–1726.

Junge, C. E. 1963. Air Chemistry and Radioactivity. Academic Press, New York, 382 pp.

Kishino, M., M. Takahashi, N. Okami and S. Ichimura. 1985. Estimation of the spectral absorption coefficients of phytoplankton in the sea. Bull. Mar. Sci., *37,* 634–642.

Koike, I., S. Hara, K. Terauchi and K. Kogure. 1990. Role of sub-micrometer particles in the ocean. Nature, *345,* 242–244.

Morel, A. 1973. Diffusion de la lumière par les eaux de mer. Résultats expérimentaux et approche théorique, *in* Optics of the Sea, AGARD Lect. Ser., *61,* 3.1.1-3.1.76.

—— 1987. Chlorophyll-specific scattering coefficient of phytoplankton, a simplified theoretical approach. Deep-Sea Res., *34,* 1093–1105.

—— 1988. Optical modeling of upper ocean in relation to its biogenous matter content (case I waters). J. Geophys. Res., *93,* N C9, 10749–10768.

Morel, A. and Y. H. Ahn. 1990. Optical efficiency factors of free living marine bacteria: Influence of bacterioplankton upon the optical properties and particulate organic carbon in oceanic waters. J. Mar. Res., *48,* 145–175.

Morel, A. and A. Bricaud. 1981. Theoretical results concerning light absorption in a discrete medium, and application to specific absorption of phytoplankton. Deep-Sea Res., *28,* 1375–1393.

—— 1986. Inherent optical properties of algal cells including picoplankton: theoretical and experimental results, *in* Photosynthetic Picoplankton, T. Platt and W. K. W. Li, eds., Can. Bull. Fish. Aquat. Sci., *214,* 521–559.

Morel, A. and L. Prieur. 1977. Analysis of variations in ocean color. Limnol. Oceanogr., *22,* 709–722.

Morrow, J. H., W. S. Chamberlin and D. A. Kiefer. 1989. A two-component description of spectral absorption by marine particles. Limnol. Oceanogr., *34,* 1500–1509.

Norland, S., M. Heldal and O. Tumyr. 1987. On the relation between dry matter and volume of bacteria. Microb. Ecol., *13,* 95–101.

Platt, T, M. Lewis and R. J. Geider. 1984. Thermodynamics of the pelagic ecosystem: Elementary closure conditions for biological production in the open ocean, *in* Flow of Energy and Materials in Marine Ecosystems: Theory and Practice. M. J. Fasham, ed., Plenum, 49–84.

Putt, M. and D. K. Stoecker. 1989. An experimentally determined carbon: volume ratio for marine "oligotrichous" ciliates from estuarine and coastal waters. Limnol. Oceanogr., *34,* 1097–1103.

Rassoulzadegan, F. and R. W. Sheldon. 1986. Predator-prey interactions of nanozooplankton and bacteria in an oligotrophic marine environment. Limnol. Oceanogr., *31,* 1010–1021.

Rivier, A., D. C. Brownlee, R. W. Sheldon and F. Rassoulzadegan. 1985. Growth of microzooplankton: a comparative study of bactivorous zooflagellates and ciliates. Marine Microbial Food Web. *1,* 51–60.

Rodriguez, J. and M. M. Mullin. 1986. Relation between biomass and body weight of plankton in a steady state oceanic ecosystem. Limnol. Oceanogr., *31,* 361–371.

Roesler, C. S., M. J. Perry and K. L. Carder. 1989. Modeling *in situ* phytoplankton absorption from total absorption spectra in productive inland marine waters. Limnol. Oceanogr., *34,* 1510–1523.

Sheldon, R. W., A. Prakash and W. H. Sutcliffe, Jr. 1972. The size distribution of particles in the ocean. Limnol. Oceanogr., *17,* 327–340.

Sherr, E. G., B. F. Sherr, R. D. Fallon and S. Y. Newell. 1986. Small, aloricate ciliates as major component of the marine heterotrophic nanoplankton. Limnol. Oceanogr., *31,* 177–183.

Sieburth, J. McN. 1983. Microbiological and organic-chemical processes in the surface and mixed layers, *in* Air-Sea Exchange of Gases and Particles, P. S. Liss and W. G. N. Slinn eds., D. Reidel Publishing Company, 121–172.

Simon, M. and F. Azam. 1989. Protein content and protein synthesis rate of planktonic marine bacteria. Mar. Ecol. Prog. Ser., *51*, 210–213.

Stramski, D. and D. A. Kiefer. 1990. Optical properties of marine bacteria. Proc. SPIE, Ocean Optics X, *1302*, 250–268.

Stramski, D. and A. Morel. 1990. Optical properties of photosynthetic picoplankton in different physiological states as affected by growth irradiance. Deep-Sea Res., *37*, 245–266.

Stramski, D., A. Morel and A. Bricaud. 1988. Modeling the light attenuation and scattering by spherical phytoplankton cells: a retrieval of the bulk refractive index. Appl. Opt., *27*, 3954–3956.

Toggweiler, J. R. 1990. Diving into the organic soup. Nature, *345*, 203–204.

Van de Hulst, H. C. 1957. Light Scattering by Small Particles. Wiley, New York, 470 pp.

Weidemann, A. D. and T. T. Bannister. 1986. Absorption and scattering coefficients in Irondequoit Bay. Limnol. Oceanogr., *31*, 567–583.